

# Large-Volume Centimeter-Wave Cavities for Axion Searches

Chao-Lin Kuo

*Kavli Institute of Particle Astrophysics and Cosmology & Physics Department,  
Stanford University, Stanford, CA 94305.*

*SLAC National Accelerator Laboratory,  
Menlo Park, CA 94025.*

(Dated: October 11, 2019)

The scan rate for an axion haloscope is proportional to the square of the cavity volume. In this paper, a new class of thin-shell cavities are proposed to search for axionic dark matter. These cavities feature active volume much larger ( $> 20\times$ ) than that of a conventional cylindrical haloscope, comparable quality factor  $Q$ , and a similar frequency tuning range. Full 3D numerical finite-element analyses have been used to show that the  $TM_{010}$  eigenmodes are singly polarized throughout the volume of the cavity and can facilitate axion-photon conversion in uniform magnetic field produced by a superconducting solenoid. To mitigate spurious mode crowding and volume loss due to localization, a pre-amplification binary summing network will be used for coupling. Because of the favorable frequency-scaling, the new cavities are most suitable for centimeter-wavelength ( $\sim 10\text{--}100$  GHz), corresponding to the promising post-inflation axion production window. In this frequency range, the tight machining tolerances required for high- $Q$  thin-shell cavities are achievable with standard machining techniques for near-infrared mirrors.

## I. INTRODUCTION

Axion, the light scalar particle that was proposed to solve the strong  $CP$  problem in QCD (quantum chromodynamics), is an excellent candidate for dark matter [1–3]. Resonant conversion to microwave photons in the presence of strong magnetic field is a mature method to search for relic QCD axions [4]. This method, known as the axion haloscope, has produced the most sensitive limits on axion coupling strength between  $0.5 - 7$  GHz, corresponding to an axion mass of  $2 - 30 \mu\text{eV}$  [5–8].

The resonator design adopted by these haloscope experiments consists of a cylindrical cavity with one or multiple vertical rod(s). The frequency tuning is achieved by rotating the off-axis rods and changing the physical configuration of the cavity. The scan rate  $dv/dt$  of an amplifier noise-limited axion haloscope is proportional to  $B_0^4 V^2 Q$ , where  $B_0$  is the applied static magnetic field,  $V$  is the *active* volume of the cavity mode coupled to the magnetic field, and  $Q$  is the quality factor of the resonator [4, 9, 10]. Since  $V$  scales as  $\nu^{-3}$ , at 10 GHz the scan rate is already down by six orders of magnitude compared to 1 GHz. This unfavorable scaling is exacerbated further by higher amplifier noise and lower quality factors achievable at higher frequencies. This represents substantial missed opportunities because an axion frequency  $\sim 10$  GHz corresponds to the important post-inflation axion generation mechanism, sometimes known as the classical window [11–13].

In recent years, there have been an explosion of new ideas on axion searches, including many new concepts that are not relying on cavities [10, 14–18]. Although this paper is focusing on the design of cavity resonators, it has certainly been partly inspired by these exciting innovations. The proposed new architecture borrows many methods well known in the cosmic microwave background (CMB) community. It can work together with novel

quantum techniques that reduce readout noise, by either operating JPAs (Josephson Parametric Amplifiers) in a squeezed setup to defeat quantum limit [19, 20], or by using photon counting Qubits or Rydberg atoms to completely circumvent it [21, 22].

In the past, there have been a few exploratory studies on alternative cavity designs. The dominant idea is to combine data from multiple cavities or cavity cells to increase the effective volume, while fixing the resonant frequency in the desired range [23–25]. Implementations of these ideas often face significant challenges in synchronous tuning. Another idea is to employ TE modes in long rectangular cavities [26]. The main disadvantage of this approach is that the linear geometry leads to substantial difficulties in cryogenics and magnetic coupling. Their recent proposal is to break this cavity into multiple cells, essentially going back to the first idea.

In this paper, a class of novel thin-shell cavities are proposed for axion searches in the few to tens of GHz (centimeter-wavelength) frequency range. The active volume of the new designs scales much more mildly, as  $\propto \nu^{-1}$ , or even weaker if a more elaborate variety can be realized. Unlike the linear resonators, this more compact design fits inside a reasonably-sized cryostat and eases difficulties in magnetic coupling. Finite-element analyses (FEA) based on COMSOL-RF have been used to verify the resonant frequencies of the linearly polarized  $TM_{010}$  mode, as well as the high quality factor of the new design. At 15 GHz ( $\lambda = 2$  cm), the active volume of a circular thin-shell design is more than 20 times that of a scaled Haystack cylindrical cavity, corresponding to a  $>400\times$  improvements in the scan rate. In principle, the active volume is only limited by practicalities, including fabrication tolerances, spatial localization of the desired mode, and mode crowding by other resonances. A phase-matching binary summing network similar to the ones used successfully in millimeter-wave astronomy is pro-

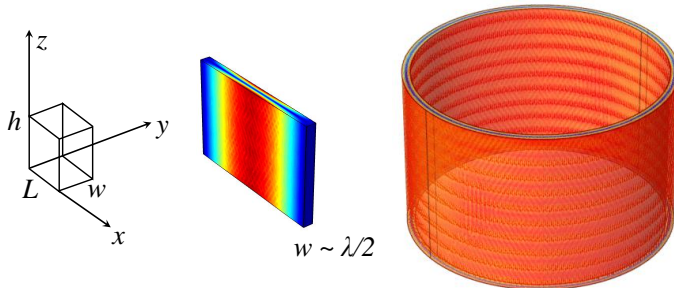


FIG. 1. *Left*: A rectangular resonant cavity. This simple cavity supports a  $\text{TE}_{110}$  mode that is polarized in the  $z$  (vertical) directions. *Center*: A rectangular cavity with extended dimensions in  $L$  and  $h$ , and a smaller  $w$ . According to Eq. (1) the  $\text{TE}_{110}$  mode (shown as surface current distribution) now resonates at  $\sim c/2w$ . *Right*: A thin-shell cavity formed by turning a rectangular cavity that has very extended  $L$  and  $h$ , with its  $x$  axis rolled up into a circle. FEA verifies the intuitive guess that this shell cavity supports a  $z$ -polarized resonance. The surface current distribution calculated by COMSOL is shown.

posed to mitigate these issues. Such summing network can ensure that the desired eigenmodes do fill the entire cavity volume and the spurious modes are rejected.

The rest of the paper is organized as the following: Section II discusses the resonant properties of the thin-shell cavities, Section III discusses practical issues, including fabrication, and a mode-managing binary summing network, Section IV covers aspects of magnetic coupling and frequency tuning. Section V discusses projected sensitivity to QCD axions and summarizes the paper.

## II. GEOMETRY AND PROPERTIES OF LARGE-VOLUME RESONATORS

The axion field interacts with a static magnetic field and creates an effective oscillatory current  $j_a$  that excites a cavity eigenmode by coupling to the  $E$  field [4, 9, 10]. Therefore, for a uniform external  $B$  field the appropriate eigenmode should be linearly polarized. We start by reviewing resonant behaviors in a simple rectangular cavity with linear dimensions  $(L, w, h)$  in the  $(x, y, z)$  directions (FIG. 1). The  $\text{TE}_{lmn}$  modes have resonant frequencies given by

$$\nu_{lmn} = \frac{c}{2} \sqrt{(l/L)^2 + (m/w)^2 + (n/h)^2}, \quad (1)$$

where  $c$  is the speed of light and  $(l, m, n)$  are non-negative integers [27]. If the external magnetic field is applied in the  $z$  direction (along  $h$ ), the  $\text{TE}_{110}$  mode is most suitable for axion searches because of its uniform polarization. In this case, the  $E$  field distribution is sinusoidal

across  $L$  and  $w$ , and uniform across  $h$ . For this mode, the resonant frequency approaches a fixed value when  $L$  and  $h$  are taken to be much larger than  $w \sim \lambda/2$ , and the cavity still resonates at  $c/\lambda$  as its volume ( $V = Lwh$ ) going to infinity.

In [26], the dimension  $L$  is taken to be the full length (a few m) of an existing dipole magnet system at CERN. In that proposal, the height  $h$  must fit inside a small gap between the dipole magnets. While the volume of this pencil beam cavity is indeed large for the frequency, the extreme geometry presents significant challenges in magnetic coupling and in cryogenics [24].

In the proposed new design,  $h$  and  $L$  are *both* taken to be much larger than  $w = \lambda/2$ , and additionally the  $L$  dimension is rolled up into a circle. The  $\text{TE}_{110}$  mode is turned into a  $\text{TM}_{010}$  mode living in a thin shell as the  $x$  axis becomes  $\phi$  and  $y$  becomes  $\rho$ . The eigenmode can be seen as a  $z$ -polarized quasi-plane wave bouncing back and forth between the inner and outer walls, setting up a standing wave (FIG. 1, *right*).

A representative circular shell resonator that resonates at 15 GHz has an inner radius  $r$  of 15 cm, an outer radius of  $r + \lambda/2 = 16$  cm, and a height  $h$  of 20 cm (FIG. 2, *left*). COMSOL-based FEA's confirm the existence of a linearly polarized  $\text{TM}_{010}$  mode sitting at 15.0 GHz in the new cavity. Incidentally, the new geometry can also be obtained by increasing *both* the inner radius  $r$  of a legacy cylindrical cavity and the radius of its tuning rod, while maintaining the gap to be  $\sim \lambda/2$ . To compare the active volume of a legacy resonator with the new thin shell design, we can scale down the Haystac cavity [28] by a factor of 2.57 in all dimensions (FIG. 2, *center top*), so that the highest resonant frequency is also at 15 GHz (confirmed by FEA). The two cavities have nearly identical form factors for the  $\text{TM}_{010}$  mode. We see that the new design has a volume that is 20.9 times larger than the scaled Haystac resonator. The larger volume represents a very significant enhancement in the scan rate, since  $d\nu/dt$  is proportional to  $V^2$ .

Another important quantity, the quality factor  $Q$ , remains about the same even as the transverse dimensions are inflated. It is easy to see that in the new thin-shell design the surface current loss is dominated by the inner and outer walls (FIG. 1), which have a total area  $A$  proportional to the volume ( $V \sim Aw$ ). Therefore, the  $Q$ -factor, which is given by the ratio of the volume and the surface loss [27], largely stays the same as  $r$  and  $h$  (and therefore  $V$ ) increase indefinitely. Numerical calculations showed that in designs where  $r \sim h \gg w$ , the  $Q$ -factors are modestly higher than that of a single-rod cylindrical cavity.

The unlimited transverse dimensions of a quasi-plane wave can be exploited further, by going into the radial dimension with structures that resemble the cerebral cortex (FIG. 2, *right*). The volume of this cavity could be nearly independent of the frequency as the number of folds increases. As long as the inter-wall distance is fixed at  $\lambda/2 = 1$  cm, this cavity should have a resonance at 15

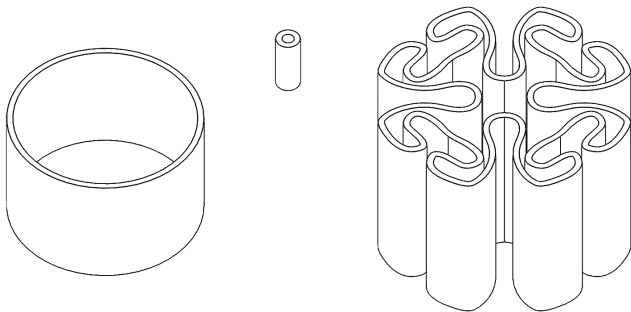


FIG. 2. *Left*: A circular thin shell cavity ( $r=15$  cm,  $h=20$  cm,  $w=1$  cm) is 20.9 times larger in volume than a conventional cylindrical cavity at the same frequency (*center top*), with a similar quality factor. This quasi-planar standing wave concept can be exploited further to improve the scan rate by an even larger factor, if the “brain” type cavity (*right*) can be fabricated with sufficient tolerances.

GHz and similar  $Q$  based on the arguments given above. The particular cavity shown has an active volume that is more than 100 times larger than a scaled cylindrical cavity. Such a “brain” cavity would be even more difficult to meet the tolerance requirements, although the factor of  $> 10^4$  improvement in scan speed should serve as a strong motivation to try. A cavity with this geometry is difficult even to simulate with FEA, however analytic treatments under WKB assumptions ( $\partial_{\perp}\psi \gg \partial_{\parallel}\psi$ , where  $\psi$  is any field quantity) should be quite straightforward. Once again, the intuitive picture is a linearly polarized quasi-plane wave bouncing back and forth between two walls.

It is rather obvious that the proposed topological (FIG. 1) and homeomorphic (FIG. 2) gymnastics would lead to high- $Q$  cavities with indefinitely large active volume, because a linearly polarized quasi-plane wave has two extended transverse dimensions. It is also apparent that the resonant frequency of a single-rod cylinder is determined by the gap between the tuning rod and the inner wall ( $\sim \lambda/2$ ). Therefore, a large-volume resonator is available simply by increasing the diameter of the rod and the cavity ID *together*.

To our knowledge, no cavity geometries similar to those depicted in FIG. 2 have been proposed in the past. Nevertheless, the main challenges for overmoded cavities are already well known in the community, *e.g.*, see [10] for a recent comprehensive review. They are (1) fabricating the cavities with sufficient machining tolerances; (2) controlling the spatial distribution of the desired eigenmodes over a volume much larger than  $\lambda^3$ ; and (3) mitigating mode crowding caused by the large volume. Although the proposed new resonators are topologically identical to a single-rod cylindrical resonator, new frequency-tuning schemes are needed to deal with the extreme geometries. In the next two sections, these issues will be discussed in greater detail.

### III. FABRICATION, COUPLING, AND OTHER IMPLEMENTATION ISSUES

To support a high- $Q$   $TM_{010}$  resonance the distance between the walls must be maintained at  $\lambda/2$  to a precision of  $\sim \lambda/2Q$  throughout the cavity. At 15 GHz and  $Q \sim 1.5 \times 10^4$ , this corresponds to a machining tolerance of  $\sim 0.7 \mu\text{m}$ . This is about the required precision for near-infrared mirrors and are routinely achieved using single-point diamond turning on stress-free metal blocks. The metal (*e.g.* nickel) parts can then be plated with high purity copper. Precision cylindrical grinding may be able to achieve the required tolerances for the circular thin shell.

Once fabricated, the spatial distribution of the cavity  $TM_{010}$  mode can be systematically surveyed using the ingenious “bead mapping” measurements described in [29], in which a dielectric bead suspended by Kevlar threads is raster-scanned in the cavity space and the corresponding frequency shifts in the resonance is used to measure the  $E$  field strength. One can imagine constructing a circular thin-shell resonator (or even a brain type resonator) out of multiple adjustable, diamond-turned panels and use the bead-mapping data to adjust the locations of the panels.

In addition, we can use a (pre-amplification) phase-coherent summing network to mitigate undesired mode crowding and spatial localization caused by remaining fabrication errors and misalignments. The large active area inevitably leads to mode crowding because it supports a large number of resonances. All the  $TM_{l1n}$  modes resonate at only slightly higher frequencies than that of  $TM_{010}$ . Furthermore, for each  $TM_{l1n}$  mode, there is a corresponding  $TE_{l1n}$  at a similar frequency. On top of all this, a very large number of TEM-like modes can exist around the frequency of the  $TM_{010}$  mode.

Fortunately, these spurious modes can be simulated and analyzed. Using FEA, we observe that of these modes only the TM modes are polarized in the vertical ( $z$ ) direction. Therefore, the first line of defense against resonance crowding by TEM-like ( $\rho$ -polarized) and TE-like ( $\phi$ -polarized) modes is to use a polarization-selective iris (elongated rectangular aperture) to couple to the cavity.

Higher order (whispering gallery)  $TM_{l1n}$  modes do have the right polarization to leak through the iris. Although they show up at frequencies higher than the desired  $TM_{010}$  mode, the mode density can be very high, leading to confusion. We propose to use a pre-amplification phase-matching summing network to (critically) couple to the cavity as a way to monitor and mitigate mode crowding by higher order  $TM_{l1n}$  and spatial localization of the  $TM_{010}$ . The binary summing network couples equally to the  $2^N$  ports with the same propagation length, where  $N$  is the number of levels. To understand how this guards against unwanted coupling, imagine in the reciprocal picture in which a signal is launched from the main branch, only the desired  $TM_{010}$  mode will

be excited. Most of other modes will be suppressed by phase cancellation. With sufficiently large number of ports, the only modes (“grating lobes”) that can still add coherently to produce a signal at the main output branch necessarily will have much higher resonant frequencies.

Another important function of this multi-port coupling scheme is to monitor against field localization. Fabrication defects lead to degeneracy breaking and undesired mode localization. For example, if the distance between the inner and outer walls is slightly larger at the top, a single  $\text{TM}_{010}$  resonance will split into two modes, localized at the top and bottom halves respectively. A single pick-up antenna located near the top of the cavity would only capture half of the active volume, and miss most of the sensitivity provided by the other new resonance now at a slightly higher frequency. This effectively reduces the active volume (form factor) of an axion haloscope.

The multi-port coupling scheme can mitigate that. Before the summing tree is connected, the off-diagonal scattering parameters of the  $2^N$  ports can be measured. At the resonant frequency the  $S_{ij}$  should all be identical both in amplitude and in *phase*. Even if mode localization persists, the spatially distributed ports can pick up all the localized modes at the fine structure frequencies so that the speed loss is only modest. This phase-sensitive method should be complementary to the bead-mapping measurements.

We should recall that the cold summing network is located outside the resonator. Therefore, the loss in the network represents slight signal attenuation and does not degrade the  $Q$ -factor. From past experiences, this somewhat complicated sounding scheme is actually quite manageable up to about 100 GHz (3 mm) for  $N \sim 5$ , or having 32 coupling ports. An example for the similar architecture is the LO distribution networks used in CMB interferometers. Also, a spatial content-controlling pre-detection summing tree has been adopted very successfully in the detectors used for the BICEP/Keck program up to 270 GHz [30].

#### IV. MAGNETIC COUPLING AND FREQUENCY TUNING

Achieving high magnetic field strength over a large volume is one of the biggest challenges in an axion experiment. Therefore, a very appealing property of the new thin-shell geometry is that it can be placed in a conventional solenoid magnet with uniform field. For example, the ADMX main cavity space can readily house a circular thin-shell cavity that resonates at higher frequencies. This will be explored further in Section V.

On the other hand, if circular thin-shell cavities can be built with even larger diameters, they are most effectively coupled to pairs of nested Helmholtz coils. One can arrive at this configuration by moving half of the superconducting wires that would have been used to complete the solenoid magnet to inside the shell cavity. To first

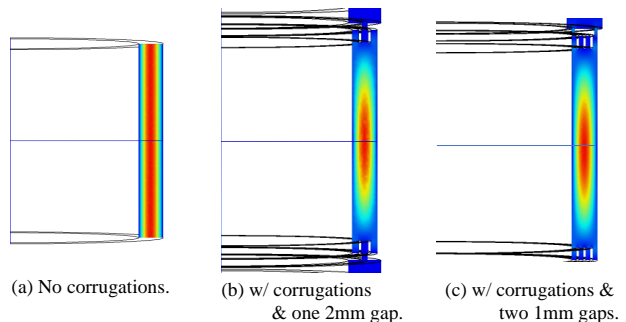


FIG. 3. Sub-wavelength corrugations ( $\lambda/4$ ) force  $E_z$  (shown in color) to vanish at the boundaries, which allow gaps to exist without disrupting the eigenmodes. These circular gaps in the top/bottom rings separate the cavity into disjoint pieces that enable frequency tuning. With one gap (*center*) the inner tube can be moved sideways or deformed; with two gaps (*right*) the top ring can be lower to reduce the height of the resonator.

order, the magnetic field achieved in the cavity shell is comparable for the same amount of current and turns. However, an added benefit is that the counter-flowing current in the inner coils significantly reduces the field strength in the central region. Away from the shell cavity/coils, the field strength drops off quickly. This will ease the engineering effort associated with quench prevention. The disadvantage of doing that is the magnets must now reside in the receiver cryostat and have to be custom-made.

Another important aspect of an axion haloscope is frequency-tuning. The proposed cavities are similar to the single-rod cavity in Haystack and can be tuned in a similar manner. To achieve sufficient tuning in the circular thin-shell cavity, we can split the top/bottom rings at the center circles and to create a  $\sim \lambda/10$  “tuning gap” to work with. The inner wall assembly then can be moved laterally by *e.g.* a piezo nanopositioner, emulating the rotation of a single off-axis tuning rod. Alternatively, the inner tube can be physically deformed by an actuator into an ellipse, emulating the effects of two offset tuning rods. Similar to the Haystack/ADMX cavities, the broken azimuthal symmetry leads to some mode localization and some volume reduction.

There is a key implementation complication. Before the split, the  $\text{TM}_{010}$  mode induces zero surface current at the fault lines due to symmetry (FIG. 3a). However, if the cavity is simply split into two disjoint halves, the surface current on each side of the gaps can flow out vertically, effectively breaking the resonator. Fortunately, this problem can be eliminated by adding azimuthal quarter-wave deep corrugations to the top and bottom rings, since such structure forces  $E_{\perp}$  (and therefore voltage build-up) to vanish at the boundaries. The corrugations convert the original uniform  $z$ -distribution into having a sinusoidal dependence while maintaining its linear polariza-

tion. The cavity now looks like a corrugated rectangular cavity (that supports a high- $Q$   $\text{HE}_{111}$  mode) squeezed in the propagation direction and rolled up into a circle in an aperture dimension [31]. FEA calculations showed that the  $Q$ -factor of the grooved cavity increases by a modest amount (8%), not quite enough to make up the loss in the form factor (factor of  $\sim 2/\pi$ ). However, as shown these full 3D calculations, these corrugations kill off the  $E$  field and the current at the top/bottom, and allow (sub-wavelength) gaps to exist for frequency tuning (FIG. 3b).

The newly created  $z$ -dependence by the corrugations also allows frequency tuning by changing the vertical configuration. This can be done either by moving the top (now corrugated) “lid” down, or by inserting a sapphire slab into the cavity space. Again, since the surface current already drops to zero near the corrugations, the gaps that are needed to mechanically realize the motion do not disrupt the cavity modes (FIG. 3c). Using Equation (1) (which is also appropriate for  $\text{HE}_{11}$  modes for oversized apertures), we see that 10% frequency tuning is achieved by reducing the cavity height from  $5\lambda$  to  $2\lambda$ . This tuning scheme leads to disproportional reduction in volume, which is undesirable. However, mode localization mentioned above is avoided because azimuthal symmetry is completely maintained during tuning. Another advantage is that this scheme can work for the brain type cavity, which offers maximal increase in the volume and hence the scan rate. Different dielectric tuning options are being studied and will be published in a follow-up work.

## V. PROJECTED SENSITIVITY AND SUMMARY

Following the standard practice in CMB research, we will use actual achieved performance, instead of idealized first-principle calculations, to project the scan rate of a benchmark haloscope program based on circular thin-shell cavities.

Recently, Haystac experiment reported a limit on axion coupling strength at a factor of 2.7 above the benchmark KSVZ model [9, 12] in the frequency range of 5.6 and 5.8 GHz. Obtained with a total of 240 days of data taking [7], this corresponds to a scan rate of 18 MHz/year for reaching KSVZ and will serve as the baseline for the scaling.

The hypothesized pathfinder haloscope program will use a series of circular thin-shell cavities covering the frequency range between 5 and 10 GHz, each filling up to the inner diameter and the height of the ADMX cavity [32]. At 5 GHz, this thin-shell cavity will have a factor of 15 larger active volume (including the form factor reduction from corrugations), or 225 times the scan rate of Haystac, if everything else is held the same. At  $\nu > 5$  GHz, the higher axion mass leads to an enhanced scan rate  $\propto \nu^2$ . However, this scan rate enhancement will be hit by a factor of  $V^2 \propto \nu^{-2}$  from the shell width reduction ( $w = \lambda/2$ ), and another factor of  $\nu^{-2/3}$  from the anomalous skin effect that reduces  $Q$ . Finally, there is the degradation in the scan rate from the amplifier standard quantum limit, incurring another factor of  $\nu^{-2}$ .

Taken together, the scaled scan rate is approximately  $d\nu/dt = 4.0(\nu/5.7\text{GHz})^{-8/3}$  GHz/year. The integral  $\int_5^{10} (d\nu/dt)^{-1} d\nu$  equals 2.8 years. In other words, it takes about three years to cover the frequency between 5 and 10 GHz to KSVZ sensitivity using quantum-limited amplifiers as readout, not including warm-up/cool-down time required for swapping shell cavities and readout systems.

This simple estimate shows the great potential of thin-shell cavities for axion searches even at the low frequency end of cm wavelength. Serious R&D efforts into fabrication and coupling issues will be very well justified.

## ACKNOWLEDGMENTS

The author acknowledges the support of a KIPAC Innovation Grant and useful discussions with Zeesh Ahmed, Jamie Bock, Ari Cukierman, Peter Graham, Kent Irwin, Jeff McMahon, and Sami Tantawi.

- 
- [1] R. Peccei and H. Quinn, *Phys. Rev. Lett.* **38**, 1440 (1977).
  - [2] S. Weinberg, *Phys. Rev. Lett.* **40**, 223 (1978).
  - [3] F. Wilczek, *Phys. Rev. Lett.* **40**, 279 (1978).
  - [4] P. Sikivie, *Phys. Rev. Lett.* **51**, 1415 (1983).
  - [5] N. Du, N. Force, R. Khatiwada, E. Lentz, R. Ottens, L. J. Rosenberg, G. Rybka, G. Carosi, N. Woollett, and D. B. et al. (ADMX Collaboration), *Phys. Rev. Lett.* **120**, 151301 (2018).
  - [6] B. M. Brubaker, L. Zhong, Y. V. Gurevich, S. B. Cahn, S. K. Lamoreaux, M. Simanovskaia, J. R. Root, S. M. Lewis, S. A. Kenany, and K. M. Backes, *Phys. Rev. Lett.* **118**(6), 061302 (2017).
  - [7] S. A. K. L. Zhong, K. Backes, B. Brubaker, S. Cahn, G. Carosi, Y. Gurevich, W. Kindel, S. Lamoreaux, and K. L. et al, *Phys. Rev. D* **97**, 092001 (2018).
  - [8] C. Boutan, M. Jones, B. H. LaRoque, N. S. Oblath, R. Cervantes, N. Du, N. Force, S. Kimes, R. Ottens, and L. J. R. et al (ADMX Collaboration), *Phys. Rev. Lett.* **121**, 261302 (2018).
  - [9] P. Graham, I. G. Irastorza, S. K. Lamoreaux, A. Lindner, and K. A. van Bibber, *Annu. Rev. Nucl. Part. Sci.* **65**, 485 (2015).
  - [10] I. G. Irastorza and J. Redondo, *Progress in Particle and Nuclear Physics* **102**, 89 (2018).
  - [11] M. Hertzberg, M. Tegmark, and F. Wilczek, *Phys. Rev. D.* **78**, 083507 (2008).
  - [12] D. J. E. Marsh, *Physics Report* **643**, 1 (2016).
  - [13] P. W. Graham and A. Scherlis, *Phys. Rev. D* **98**, 035017

- (2018).
- [14] S. Chaudhuri, P. W. Graham, K. Irwin, J. Mardon, S. Rajendran, and Y. Zhao, *Phys. Rev. D.* **92**, 075012 (2015).
- [15] D. Budker, P. Graham, M. Ledbetter, S. Rajendran, and A. Sushkov, *Phys. Rev. X.* **4**, 021030 (2014).
- [16] Y. Kahn, B. Safdi, and J. Thaler, *Phys. Rev. Lett.* **117** (14), 141801 (2016).
- [17] P. Sikivie, N. Sullivan, and D. Tanner, *Phys. Rev. Lett.* **112**(13), 131301 (2013).
- [18] A. Ioannisian, N. Kazarian, A. Millar, and G. Raffelt, *J. Cosmol. Astropart. Phys.* **1709(09)**, 005.
- [19] S. Lamoreaux, K. van Bibber, K. Lehnert, and G. Carosi, *Phys. Rev. D* **88**, 035020 (2013).
- [20] H. Zheng, M. Silveri, R. Brierley, S. Girvin, and K. Lehnert, arXiv:1607.02529. (2016).
- [21] A. Dixit, A. Chou, and D. Schuster, *Springer Proc. Phys.* **211**, 97 (2018).
- [22] M. Shibata, T. Arai, A. Fukuda, H. Funahashi, T. Haseyama, S. Ikeda, K. Imai, Y. Isozumi, T. Kato, and Y. K. et. al., *Journal of Low Temperature Phys.* **151** (3-4), 1043 (2008).
- [23] J. Jeong, S. Youn, S. Ahn, C. Kang, and Y. K. Semertzids, *Astropart. Phys.* **97**, 33 (2017).
- [24] A. . Melcn, S. A. Cuendis, C. Cogollos, A. Daz-Morcillo, B. Dbrich, J. D. Gallego, B. Gimeno, I. G. Irastorza, A. J. Lozano-Guerrero, and C. M. et. al., *JCAP* **05**, 40.
- [25] B. T. McAllister, G. Flower, J. Kruger, E. N. Ivanov, M. Goryachev, J. Bourhill, and M. E. Tobar, *Phys. Dark Univ.* **18**, 67 (2017).
- [26] O. Baker, M. Betz, F. Caspers, J. Jaeckel, A. Lindner, A. Ringwald, Y. Semertzidis, P. Sikivie, and K. Zioutas, *Phys. Rev. D* **85**, 035018 (2012).
- [27] C. A. Balanis, *Advanced Engineering Electromagnetics*, 2nd ed. (John Wiley & Sons, Inc., 2012).
- [28] B. M. Brubaker, PhD dissertation, Yale University, Department of Physics (2018).
- [29] S. A. Kenany, M. A. Anil, K. M. Backes, B. M. Brubaker, S. B. Cahn, G. Carosi, Y. V. Gurevich, W. F. Kindel, S. K. Lamoreaux, and K. W. L. et. al., *Nucl. Instrum. Methods A* **854**, 11 (2017).
- [30] C. L. Kuo, J. J. Bock, J. A. Bonetti, J. Brevik, G. Chatopadhyay, P. K. Day, S. Golwala, M. Kenyon, A. E. Lange, and H. G. L. et. al., *SPIE Proceedings, Millimeter and Submillimeter Detectors and Instrumentation for Astronomy IV* **7020**, arXiv:0908.1464 (2008).
- [31] C. Dragone, *IEEE Trans. on Microwave Theory and Tech.* **MTT-28 No 7**, 704 (1980).
- [32] D. Lyapustin, PhD dissertation, University of Washington, Department of Physics (2015).